

STABLE CRACK GROWTH ESTIMATES BASED ON EFFECTIVE  
CRACK LENGTH AND CRACK-OPENING DISPLACEMENT\*

J. G. Merkle  
Oak Ridge National Laboratory  
Oak Ridge, Tennessee 37830

C. E. Hudson<sup>†</sup>  
Auburn University  
Auburn, Alabama

## NOTICE

This report was prepared as an account of work sponsored by the United States Government. Neither the United States nor the United States Department of Energy, nor any of their employees, nor any of their contractors, subcontractors, or their employees, makes any warranty, express or implied, or assumes any legal liability or responsibility for the accuracy, completeness or usefulness of any information, apparatus, product or process disclosed, or represents that its use would not infringe privately owned rights.

MASTER

## ABSTRACT

A method has been developed for estimating the amount of stable crack growth that has occurred in a fracture toughness specimen that has been loaded into the plastic range and for which only a monotonically increasing load-displacement curve has been measured. The method has been applied to data from several pressure vessel steels. The resulting  $J$  vs  $\Delta a$  values compare favorably with a resistance curve obtained by the multiple specimen heat-tinting technique for A533, Grade B, Class 1 steel. The method for estimating stable crack growth uses several existing concepts heretofore mainly used separately. These concepts include an approximate expression for  $J$  for the compact specimen proposed by Andrews, the effective crack length concept of McCabe and Landes, the UK representation of the crack profile as a pair of straight lines intersecting at a hinge point, and Well's expression,  $J = m\sigma_y\delta$ , for relating the crack-opening displacement to the value of  $J$ . The value of the constraint factor,  $m$ , at the advancing crack tip is estimated by means of a relation between ductility and fracture toughness. When calculated with respect to the COD at the original fatigue crack tip, the constraint factor,  $m_0$ , is found to have a value consistently close to 2.0 for compact and

\*Research sponsored by Office of Nuclear Regulatory Research, U.S. Nuclear Regulatory Commission under Interagency Agreements 40-551-75 and 40-552-75 with the U.S. Department of Energy under contract W-7405-eng-26 with the Union Carbide Corporation.

<sup>†</sup>Work performed during Co-op assignment in the Metals and Ceramics Division, Oak Ridge National Laboratory.

By acceptance of this article, the publisher or recipient acknowledges the U.S. Government's right to retain a nonexclusive, royalty-free license in and to any copyright covering the article.

## **DISCLAIMER**

**This report was prepared as an account of work sponsored by an agency of the United States Government. Neither the United States Government nor any agency Thereof, nor any of their employees, makes any warranty, express or implied, or assumes any legal liability or responsibility for the accuracy, completeness, or usefulness of any information, apparatus, product, or process disclosed, or represents that its use would not infringe privately owned rights. Reference herein to any specific commercial product, process, or service by trade name, trademark, manufacturer, or otherwise does not necessarily constitute or imply its endorsement, recommendation, or favoring by the United States Government or any agency thereof. The views and opinions of authors expressed herein do not necessarily state or reflect those of the United States Government or any agency thereof.**

## **DISCLAIMER**

**Portions of this document may be illegible in electronic image products. Images are produced from the best available original document.**

precracked Charpy specimens. The method of estimation requires no auxiliary load-deflection measurements or calculations, and so permits single specimen estimates of stable crack growth to be made without the necessity of making high precision unloading compliance measurements.

## INTRODUCTION

The useful application of fracture mechanics to the safety analysis of nuclear pressure vessels has been considerably enhanced by the development of elastic-plastic methods for measuring high values of fracture toughness with small specimens,<sup>1-3</sup> and by the high safety margins demonstrated by the intermediate pressure vessel tests conducted by the HSST Program.<sup>4</sup> Nevertheless, two aspects of these results still require additional clarification before standard methods of elastic-plastic fracture toughness measurement and flaw evaluation can be considered appropriate. The first aspect is the tendency for maximum load fracture toughness values in the upper shelf temperature range to increase with increasing specimen size. The second aspect is the occurrence of relatively large amounts of stable crack growth before failure in the upper shelf intermediate pressure vessel tests. In addition, because of space limitations and other size-related problems, only small specimens can be used as irradiation surveillance specimens in reactor pressure vessels. Consequently, there is no practical alternative to the use of small specimens for measuring irradiated fracture toughness values. Furthermore, in order to justify the use of such values in fracture safety analyses, it is first necessary to explain their physical basis and also to develop procedures for using them analytically that do not become unconservative.

The physical basis for the occurrence of maximum load toughness values that increase with increasing specimen size was shown by Griffith<sup>5</sup> to be the amount of stable crack growth that occurs prior to maximum load. Griffith's<sup>5</sup> data showed that the absolute amount of stable crack growth occurring at maximum load, for notched bend specimens of HY-180 steel, increased with increasing

specimen size, although the fractional value decreased slightly, from about 6% for a 1.6-mm-thick specimen to about 4% for a 53-mm-thick specimen. On the other hand, the toughness at the onset of crack extension was about constant for specimens exceeding about 2 cm in thickness. If the toughness required to develop stable crack extension is indeed an increasing and a single valued function of the amount of stable crack growth,<sup>6</sup> then it follows that to justify using values of fracture toughness higher than those corresponding to the onset of crack extension, the amount of stable crack growth as well as the toughness must be determined from specimen test data, and both values must be used for a correct safety analysis of a flawed structure.

Multiple direct or indirect measurements of stable crack growth in single specimens are not easily made, for a variety of reasons. One method for estimating stable crack extension that is considered potentially applicable to irradiated specimens, but that also illustrates the precision problems associated with auxiliary crack length measurements, is the unloading compliance method.<sup>7</sup> By this method, the specimen is partially unloaded from the elastic-plastic range, and the crack length is calculated from the change in the elastic unloading compliance and the known elastic compliance of the specimen as a function of crack length.<sup>7</sup> Because the change in compliance due to a given change in crack length is inversely proportional to the specimen size,<sup>7</sup> it can be estimated that to prevent errors in the value of the toughness at the onset of crack extension from exceeding 10% for a 4T compact specimen, which is used in research for obtaining baseline data, the unloading displacement must be measured within 30  $\mu$ in. Consequently, efforts are underway to improve the precision and the accuracy of unloading displacement measurements, and simultaneously to develop alternate means for estimating small amounts of stable crack extension without the requirement of unloading. Andrews et al.<sup>8</sup> at the General Electric Company have proposed such a method, based on two crack opening displacement measurements made at different distances from the crack tip, from which the opening displacement at the original fatigue sharpened crack tip can be calculated. By correlation, the difference between this displacement and the displacement at the same location that would have occurred if there had been no crack extension are used to estimate the amount of stable crack extension. Another method has been proposed by Paris et al.,<sup>9</sup> based on the analytical or experimental determination of the family of load-displacement curves for specimens of constant crack length, covering the

range from initial to final crack sizes occurring in the specimen. Both of these methods are still under development and therefore their suitability for routine application cannot yet be judged. In the meantime, it appears worthwhile to continue exploring for other possible methods of estimating crack length changes without unloading, especially if these methods appear to be easily applied and their results promise to be reasonably accurate. This discussion describes one such possible method which, if it proves to be feasible, can be applied to any new or existing elastic-plastic fracture toughness data that include both load and either load point or front face clip gage displacement values.

#### EFFECTIVE CRACK LENGTH

In order to estimate the increase in crack length in a specimen without partially unloading the specimen or making other auxiliary additional measurements, the increase in crack length must be related to some characteristic of the measured load-deflection curve for continued loading. A relationship adaptable to this purpose was proposed by Bucci et al.,<sup>10</sup> who suggested that the secant modulus of the load-deflection curve could be estimated by adding an  $r_y$  plastic zone size correction to the original crack length, and then estimating the secant modulus as the elastic stiffness corresponding to the resulting effective crack length. Recently, McCabe and Landes<sup>11</sup> suggested reversing this procedure, so that the effective crack length is estimated from the measured secant modulus of the load-deflection curve. The latter procedure has the realistic advantage that the effective crack length cannot exceed the specimen width. Furthermore, McCabe and Landes<sup>11</sup> showed that  $J$  calculations based on the elastic formula for  $K$ , the actual load and the effective crack length were consistently close to the experimentally determined values of  $J$  defined as minus the rate of change of area under the load-deflection curve with increasing crack area, at constant deflection. This latter result turns out to be of considerable practical importance, even though there is presently no complete theoretical explanation for the result itself.

#### SINGLE SPECIMEN EQUATIONS FOR $J$

Soon after the relationship between the effective crack length and the nonlinear load-deflection curve was suggested,<sup>10</sup> equations began to be developed by

which  $J$  could be calculated from a single specimen nonlinear load-displacement test record. For the notched beam, Rice, Paris and Merkle<sup>2</sup> derived the equation

$$J = \frac{2A}{bB}, \quad (1)$$

where  $A$  is the area under the load-displacement curve,  $b$  is the ligament width, and  $B$  is the specimen thickness. Subsequently, for the compact specimen, Merkle and Corten<sup>3</sup> derived the equation

$$J = \frac{(1 + \alpha)}{(1 + \alpha^2)} \cdot \frac{2A}{bB} + \frac{\alpha(1 - 2\alpha - \alpha^2)}{(1 + \alpha^2)^2} \cdot \frac{2(P\Delta - A)}{bB}, \quad (2)$$

where  $P$  is the load,  $\Delta$  the displacement, and  $\alpha$  is the fraction of the net section that carries the applied force at limit load, and is given by

$$\alpha = \left[ \left( \frac{2\alpha}{b} \right)^2 + 2 \left( \frac{2\alpha}{b} \right) + 2 \right]^{1/2} - \left( \frac{2\alpha}{b} + 1 \right) \quad (3)$$

Note that Eq. (1), as well as Eq. (2), is written here in terms of the total displacement, in agreement with the subsequent findings of several investigators.<sup>12-14</sup> Also, in this discussion, the displacement  $\Delta$  will be the load line displacement and the area  $A$  will be the area under the load versus load line displacement, unless otherwise specified.

Recently, several investigators have proposed simplified approximations to Eq. (2) for the compact specimen. Andrews<sup>8</sup> found that the expression

$$J = \frac{3}{2 + (\alpha/W)} \cdot \frac{2A}{bB} \quad (4)$$

agrees with Eq. (2) within three to four percent, for  $\alpha/W \geq 0.5$ . On the other hand, Landes, Walker and Clarke<sup>14</sup> found that satisfactory agreement with experimentally based values of  $J$ , for a series of blunt notched compact specimens of

HY-130 steel, could be obtained by using only the first term in Eq. (2), that is, by writing

$$J = \frac{1 + \alpha}{1 + \alpha^2} \cdot \frac{2A}{bB} . \quad (5)$$

Based on the same comparison between experimentally determined and calculated values of  $J$ , Clarke and Landes<sup>15</sup> have since recommended Eq. (5) as the best expression to use for determining  $J$  for the compact specimen.

Both Eqs. (4) and (5) are single term equations for  $J$  reminiscent of the equivalent energy formula<sup>1</sup> for the compact specimen, because they are both equations of the form

$$J = \frac{\lambda A}{bB} . \quad (6)$$

The difference between Eqs. (4) and (5) can be investigated by considering a general approximation for  $\lambda$  to be of the form

$$\lambda = \frac{2A_0}{B_0 + (a/W)} . \quad (7)$$

where

$$B_0 = A_0 - 1 . \quad (8)$$

An appropriate value of  $A_0$  can be determined graphically by noting that the reciprocal of  $\lambda$  is a linear function of  $a/W$ , and that, for  $a/W = 0$ ,

$$\frac{2}{\lambda} = \frac{B_0}{A_0} . \quad (9)$$

Thus by plotting the values of  $2/\lambda$  calculated from Eq. (5) versus  $a/W$ , and then fitting a straight line to the results, as shown in Fig. 1, it can be determined

that within one percent accuracy, for  $a/W \geq 0.3$ ,  $B_0/A_0 = 7/9$ , so that Eq. (5) can be represented by the expression

$$J = \frac{9}{7 + 2(a/W)} \cdot \frac{2A}{bB} \quad (10)$$

Figure 1 also shows a comparison between Eqs. (4) and (2), for the elastic case. In general, the accuracy of Eq. (4) will depend on the value of  $a/W$  and the extent of yielding. However, it can be seen from Fig. 1 that Eq. (10) is a closer approximation to Eq. (5) than Eq. (4) is to Eq. (2). In addition, Eq. (10) always gives slightly smaller values of  $J$  than Eq. (4). The difference is six percent at  $a/W = 0.5$ , and it decreases steadily as  $a/W$  increases. Consequently, the value of  $B_0 = 3.5$  will be used for subsequent calculations for the compact specimen, based on Eq. (10).

#### ENERGY AND COMPLIANCE EQUATIONS

One way of checking the accuracy of an approximate energy based expression for  $J$  is to use it to estimate the area under the load-displacement curve as a function of crack length at constant displacement. For this purpose, combining Eqs. (6) and (7) with the basic definition of  $J$  gives

$$\frac{A_0}{B_0 + (a/W)} \cdot \frac{2U}{bB} = \frac{1}{B} \frac{\partial U}{\partial a} \quad \Delta = \text{const.} \quad (11)$$

where, in accordance with common usage,  $U$  and  $A$  are synonymous. After using Eq. (8) and the substitutions

$$b = W - a \quad (12)$$

and

$$\frac{b}{W} = x, \quad (13)$$

and noting that  $U$  varies only with  $b$  if  $\Delta$  is held constant, Eq. (11) can be converted to the ordinary differential equation

$$\frac{dU}{U} = \frac{2A_0}{A_0 - x} \cdot \frac{dx}{x} . \quad (14)$$

By direct integration, the solution to Eq. (14) is

$$\frac{U}{U_0} = \left( \frac{1 - (a/W)}{1 - (a_0/W)} \right)^2 \left( \frac{B_0 + (a_0/W)}{B_0 + (a/W)} \right)^2 , \quad \Delta = \text{const.} \quad (15)$$

where  $U_0$  is the value of  $U$  at any reference value of crack size, denoted by  $a_0$ .

The predictions of Eq. (15) can be compared with experiment by first noting that the ratio of energies for two specimens of different crack lengths is independent of displacement. Therefore, at any displacement,

$$\frac{P}{P_0} = \frac{U}{U_0} . \quad (16)$$

From Eq. (16) it follows that the variation of elastic compliance with crack size can be estimated from

$$\frac{c}{c_0} = \frac{U_0}{U} , \quad \Delta = \text{const.} \quad (17)$$

The predictions of Eq. (17) are compared with the boundary collocation values obtained by Newman,<sup>16</sup> in Fig. 2, using Newman's elastic compliance values at  $a/W = 0.6$  as reference values. From Fig. 2 it can be seen that using  $B_0 = 3.5$  produces a very close estimate of Newman's front face crack mouth opening compliance curve, while  $B_0 = 2.0$  produces a more accurate estimate of the load line compliance curve than does  $B_0 = 3.5$ . Equation (16) has also been applied in the elastic-plastic range to the series of load-displacement curves for ten blunt notched compact specimens of HY-130 steel obtained by Landes, Walker and Clarke<sup>14</sup> shown in Fig. 3. Using  $B_0 = 3.5$ , the predicted loads at  $\Delta = 2 \text{ mm}$  (0.08 in.) are slightly high for  $a/W < 0.6$ , the load for which was used as the reference

value, but they are extremely good for  $a/W > 0.6$ . Since all of the comparisons made thus far indicate that Eqs. (7) and (15) are good approximations, the use of Eq. (7) in a method for estimating the extent of stable crack growth will now be examined.

### SOLUTIONS FOR THE EFFECTIVE CRACK LENGTH

At first glance, a method for reconciling the effective crack length concept of McCabe and Landes<sup>11</sup> with the area based  $J$  formulas of Andrews<sup>8</sup> and Landes et al.<sup>14</sup> is not obvious. Nevertheless, it is possible to equate the  $J$  values calculated by the two methods, and thus obtain a solution for the effective crack length. By this approach, for the compact specimen.

$$\frac{J(BW)}{A_0} = \frac{2A}{[B_0 + (a/W)][1 - (a/W)]} = \frac{P\Delta}{[B_0 + (a_e/W)][1 - (a_e/W)]}, \quad (18)$$

where  $a_e$  is the effective crack length. The expression for effective crack length obtained by rearranging Eq. (18) is

$$\frac{a_e}{W} = \frac{1}{2} \left\{ \sqrt{(B_0 - 1)^2 - 4 \left[ \frac{P\Delta}{2A} \left( B_0 + \frac{a}{W} \right) \left( 1 - \frac{a}{W} \right) - B_0 \right]} - (B_0 - 1) \right\}. \quad (19)$$

If it is assumed that the ratio  $P\Delta/A$  is the same whether based on front face or load line displacement, then  $a_e/W$  can be determined before the ratio of the two displacements is known.

To be considered useful, Eq. (19) must give estimates of effective crack length that agree with certain logical restrictions. These are that (1) for a completely linear load-displacement curve, the effective crack length should be the actual crack length,  $a$ ; (2) for large displacements at limit load, the effective crack length should not exceed the distance to the point of stress reversal; and (3) the effective crack length should not exceed the width of the specimen under any conditions. From Eq. (18) it is easily seen that requirement (1) is satisfied. To determine if requirement (2) is satisfied, Eq. (19) needs

to be evaluated for the case of  $A = P\Delta$ , and the result compared with the distance to the point of stress reversal at limit load which, based on Fig. 4, is given by

$$\frac{t}{W} = \frac{\alpha}{W} + \frac{(1 + \alpha)}{2} \left( 1 - \frac{\alpha}{W} \right), \quad (20)$$

where  $\alpha$  is given by Eq. (3). The results are given in Table 1 which indicates that for an infinite displacement at limit load, the effective crack tip approaches the neutral axis, but remains within the tensile yielding zone. For either  $a/W = 1$ , which is the extreme limit for a very deep crack, or  $P\Delta/2A = 0$ , which is the extreme limit for a point on the load-displacement curve well past maximum load, Eq. (19) reduces to  $a_e/W = 1$ , indicating that requirement (3) is satisfied.

The solution for the effective crack length in a notched beam is even more straightforward. Combining the area based<sup>2</sup> and the effective crack length<sup>11</sup> equations for  $J$  gives

$$J = \frac{2A}{bB} = \frac{P\Delta}{b_e B}, \quad (21)$$

where  $b_e$  is the effective ligament length. From Eq. (21) it follows that

$$\frac{b_e}{b} = \frac{P\Delta}{2A}. \quad (22)$$

For elastic behavior,  $P\Delta/2A = 1$  and  $b_e = b$ . For an infinite displacement at limit load,  $P\Delta/2A = 1/2$  and  $b_e = 1/2 b$ . At the end of the descending branch of the load-displacement curve,  $P\Delta/2A = 0$  and  $b_e = 0$ . Thus requirements (1), (2), and (3) are all satisfied.

#### DETERMINATION OF THE PHYSICAL INCREASE IN CRACK SIZE

The effective crack length has two components, as shown in Fig. 5. The component of main interest is the physical crack length, denoted by  $a_p$ . The remainder of the effective crack length is the intensely yielded but still intact

zone of length  $\rho$ . By utilizing the familiar although approximate assumption that the profile of each side of the effective crack surface remains a straight line, it follows from Fig. 5 that for a compact specimen

$$\frac{\rho}{\delta} = \frac{\alpha_e + z}{\Delta g} . \quad (23)$$

where  $\delta$  is the crack opening displacement at the actual physical crack tip. From Eq. (23) it follows that

$$\frac{\rho}{W} = \frac{\delta}{\Delta g} \left( \frac{\alpha_e}{W} + \frac{z}{W} \right) . \quad (24)$$

For a notched beam under three point bend loading, neglecting arm curvature,

$$\theta = \frac{\delta}{\rho} = \frac{4\Delta}{S} \quad (25)$$

where  $S$  is the span and  $\Delta$  is the displacement of the load. For a standard specimen with  $S = 4W$ ,

$$\frac{\delta}{\rho} = \frac{\Delta}{W} , \quad (26)$$

so that

$$\rho = \frac{\delta}{\Delta} W . \quad (27)$$

The value of  $\delta$  in Eqs. (24) and (27) will be determined here by using the relation between  $J$  and  $\delta$  proposed by Wells,<sup>17</sup> namely

$$J = m \sigma_Y \delta , \quad (28)$$

where  $m$  is the crack tip triaxial constraint factor. However, once stable crack growth has occurred, it is necessary to distinguish between the values of crack

opening displacement and constraint factor that exist at the actual advancing crack tip from those that pertain to the original fatigue crack tip (see Fig. 5). The former values will be denoted here by the symbols  $\delta$  and  $m$ , and the latter values by  $\delta_0$  and  $m_0$ . Values of  $m_0$  have been estimated by several different investigators. Boyle and Wells<sup>18</sup> found that, for plane strain,  $1.7 < m_0 < 2.1$ , by analyzing cracked specimens of several different geometries in plane strain. Based on other analyses, Harrison<sup>19</sup> found that  $m_0 = 1.3$  for plane stress and  $m_0 = 1.7$  for plane strain. Finally, on the basis of experimental data, Dawes<sup>20</sup> found that  $1.5 < m_0 < 2.1$ . All of the above values of  $m_0$  were determined from the equation

$$m_0 = \frac{J}{\sigma_Y \delta_0} . \quad (29)$$

However, a different problem exists here because  $m$  must be determined before  $\delta$  is known. Consequently,  $m$  must be determined from its basic definition as the ratio of the actual crack tip stress to the yield stress. Therefore, it is necessary to have a relationship between toughness and the maximum crack tip stress. The relationship to be used here is one that has already been shown to relate plane strain ductility to fracture toughness, for A533-B steel,<sup>21</sup> up to  $K_{Ic}$  values approaching  $154 \text{ MN} \cdot \text{m}^{-3/2}$  ( $140 \text{ ksi} \sqrt{\text{in.}}$ ). According to this relationship,

$$K_{Ic} = \sqrt{\pi \rho_0} \sqrt{EH\sigma_Y} (e^{s/2} - 1) \quad (30)$$

where  $\rho_0$  is the effective root radius,  $H\sigma_Y$  is the slope of the strain hardening branch of the stress-strain curve, and  $s$  is the maximum crack tip strain. For  $\rho_0 = 0.05 \text{ mm}$  (0.002 in.),  $H = 3$ ,  $\sigma_Y = 483 \text{ MPa}$  (70 ksi) and  $E = 20.68 \times 10^4 \text{ MPa}$  ( $3 \times 10^7 \text{ psi}$ ), Eq. (30) can be rearranged to read

$$s = 2 \ln \left( 1 + \frac{K_{Ic}}{220} \right) , \quad (31)$$

where  $K_{Ic}$  is expressed in  $\text{MN} \cdot \text{m}^{-3/2}$ . For inelastic conditions,  $K_{Ic}$  can be calculated from the value of  $J$ , using

$$K_{Ic} = \sqrt{EJ} . \quad (32)$$

Furthermore, for the assumed case of linear strain hardening,

$$m = 1 + Hs . \quad (33)$$

Finally, once  $m$  is known,  $\delta$  can be calculated from the equation

$$\delta = \frac{J}{m \sigma_y} \quad (34)$$

For the compact specimen, once the values of  $\delta$  and  $\rho$  are determined, the amount of stable crack extension can be calculated from

$$\Delta a = W \left( \frac{a_e}{W} - \frac{\alpha}{W} - \frac{\rho}{W} \right) . \quad (35)$$

In the case of compact specimen data consisting of load and crack mouth rather than load line displacement values, the ratio of the two displacements must be known in order to calculate  $J$ . If this ratio is assumed to be approximately constant, then it is given by

$$\frac{\Delta L}{\Delta g} = \frac{(a_e/W)}{(a_e/W) + (z/W)} . \quad (36)$$

Consequently, the value of  $J$  can be calculated from

$$J = \left( \frac{\Delta L}{\Delta g} \right) \cdot \frac{\lambda A_g}{Bb} , \quad (37)$$

where  $A_g$  is the area under the load versus front face clip gage displacement curve.

For checking purposes, the value of  $m_0$  can be calculated, once  $\Delta_L/\Delta_g$  is known. From Fig. 5,

$$\frac{\Delta_L}{\alpha_e} = \frac{\delta_0}{\alpha_e - \alpha}, \quad (38)$$

and

$$m_0 \delta_0 = m\delta. \quad (39)$$

Hence it follows, by using Eqs. (34), (38), and (39), that

$$m_0 = \frac{1}{\left[ 1 - \frac{(\alpha/W)}{(\alpha_e/W)} \right]} \cdot \frac{J}{\sigma_y \Delta_g \left( \frac{\Delta_L}{\Delta_g} \right)}. \quad (40)$$

Correspondingly, for the notched beam,

$$(\alpha_e - \alpha) = \Delta\alpha_e = b \left( 1 - \frac{b_e}{b} \right), \quad (41)$$

and

$$\Delta\alpha = \Delta\alpha_e - \rho. \quad (42)$$

Also, since, from Fig. 5,

$$\frac{\delta}{\rho} = \frac{\delta_0}{\Delta\alpha_e}, \quad (43)$$

combining Eqs. (39) and (43) gives

$$m_0 = m \left( \frac{\rho}{\Delta\alpha_e} \right). \quad (44)$$

## TRIAL CALCULATIONS

The foregoing equations were applied to several sets of experimental data for pressure vessel steels, and the results were compared for reasonableness with an available  $J - \Delta a$  resistance curve for A533-B steel.<sup>22</sup> The specimens chosen for analysis were those for which the middle region of the crack advanced in the plane of the original fatigue precrack, and for which the load-displacement diagram showed no sudden load drops. The calculations were each made for the maximum load point of a test record. Specimen types and sizes ranged from precracked Charpy V-Notch specimens to 1T compact specimens. All the specimens were loaded monotonically to a displacement past maximum load. The data analyzed are listed in Tables 2 and 3, and the results are plotted in Fig. 6.

Nine of the specimens analyzed were precracked Charpy V-Notch specimens. These data are listed in Table 2. Of these, three were from the V-7B weld repair region of HSST Program V-8 prolongation,<sup>23</sup> and six were from base plate material in HSST weldment W57.<sup>24</sup> Eleven of the specimens analyzed were compact specimens. These data are listed in Table 3. Of these, two were Charpy thickness compact specimens of A537, class 1 steel; seven were 1T specimens of the same material; one was a 1T specimen of A537, class 2 steel; and one was a 1T specimen of A508, class 1 steel.<sup>25</sup>

As shown in Fig. 6, the calculated results lie quite close to the  $J - \Delta a$  resistance curve for A533, grade B, class 1 steel.<sup>22</sup> This indicates both the reasonableness of the analysis method despite its several approximations, and the probable similarity of the resistance curves for several different pressure vessel steels of similar yield strength. It is especially noteworthy that the values plotted in Fig. 6 were obtained from single specimen test data, without any auxiliary crack length measurements, experimental data or analyses being required. In fact, stable crack growth determinations were not even planned when the original tests were performed. Most of the compact specimens were tested with load line displacement gages, but two of them (the Charpy thickness compact specimens) had only front face clip gages.

All of the specimens analyzed here were loaded monotonically to displacements beyond their maximum load points. Preliminary analysis of data from a single specimen that underwent cyclic unloading and reloading for crack length measurements indicates that such cycling may affect the crack tip constraint factor,

because of reversed yielding near the crack tip. While this may create a problem in comparing calculated results for unloading compliance specimens, it would not be involved in the analysis of monotonically loaded specimens.

#### DISCUSSION

Although the method of data analysis developed here contains several approximations, it is important to note that most of the approximations were developed by others, and have been in use separately for some time. The equation for  $J$  for the compact specimen has the same form as the equation proposed by Andrews,<sup>8</sup> and it agrees numerically with the recent proposal of Clarke and Landes.<sup>15</sup> The geometric treatment of the crack profile as a pair of straight lines intersecting at a hinge point, and the relation between  $J$  and the crack opening displacement, both agree with accepted practice in the UK.<sup>17,20</sup> The estimation of an effective crack length is taken from the recent work of McCabe and Landes,<sup>11</sup> and the assumption of a relation between ductility and fracture toughness agrees in principle with the recent EPRI sponsored work of Lawrence Livermore Laboratory<sup>26</sup> and Fracture Control Corporation.<sup>27</sup> Therefore, although it contains several different approximations, the method proposed here for estimating stable crack growth from upper shelf toughness data is consistent with several other accepted approaches and, perhaps most important of all, it is simple, both analytically and experimentally.

## REFERENCES

1. F. J. Witt and T. R. Mager, "Fracture Toughness  $K_{Icd}$  Values at Temperatures up to 550°F for ASTM A533 Grade B, Class 1 Steel," *Nuclear Engineering and Design* 17(1), 91-102 (August 1971).
2. J. R. Rice, P. C. Paris, and J. G. Merkle, *Some Further Results of J-Integral Analysis and Estimates*, pp. 231-45 in ASTM STP 536, American Society for Testing and Materials (1973).
3. J. G. Merkle and H. T. Corten, "A J-Integral Analysis for the Compact Specimen, Considering Axial Force as Well as Bending Effects," *J. of Pressure Vessel Technology* 96(A), 286-92, ASME (November 1974).
4. J. G. Merkle, G. D. Whitman, and R. H. Bryan, *An Evaluation of the HSST Program Intermediate Pressure Vessel Tests in Terms of Light-Water-Reactor Pressure Vessel Safety*, ORNL-TM-5090, Oak Ridge National Laboratory (November 1975).
5. C. A. Griffis, "Elastic-Plastic Fracture Toughness: A Comparison of J-Integral and Crack Opening Displacement Characterizations," *J. of Pressure Vessel Technology* 97(4), 278-83, ASME (November 1975).
6. J. D. Landes and J. A. Begley, "Recent Developments in  $J_{Ic}$  Testing," in *Developments in Fracture Mechanics Test Methods Standardization*, ASTM STP 632, American Society for Testing and Materials (1977).
7. G. A. Clarke, W. R. Andrews, P. C. Paris and D. W. Schmidt, *Single Specimen Tests for  $J_{Ic}$  Determination*, ASTM STP 590, American Society for Testing and Materials, pp. 27-42 (1976).
8. W. R. Andrews, "Experimental Investigations in Plastic Fracture," Section 4 in *Fifth Quarterly Report to EPRI on Methodology for Plastic Fracture*, C. F. Shih et al. authors, SRD-77-165, General Electric Company, Schenectady, NY (Nov. 1, 1977).
9. H. Ernst, P. C. Paris, M. Rossow and J. W. Hutchinson, "The Analysis of Load-Displacement Relationships to Determine J-R Curve and Tearing Instability Material Properties," presented at *Conference on Concepts in Elastic-Plastic Fracture Mechanics*, Washington University, St. Louis, Mo., May 31-June 2, 1978.
10. R. J. Bucci, P. C. Paris, J. D. Landes, and J. R. Rice, *J-Integral Estimation Procedures*, ASTM STP 514, Part II, American Society for Testing and Materials, pp. 40-69 (1972).
11. D. E. McCabe and J. D. Landes, "An Evaluation of Elastic-Plastic Methods Applied to Crack Growth Resistance Measurement," paper presented at the ASTM Committee E-24 Symposium on *Elastic-Plastic Fracture*, Atlanta, Georgia, Nov. 16-18, 1977.

12. J. E. Srawley, "On the Relation of  $J_I$  to Work Done Per Unit Uncracked Area: 'Total,' or Component 'Due to Crack,'" *Int. J. of Fracture* 12(3), 470-74 (June 1976).
13. H. P. Keller and D. Munz, "Comparison of Different Equations for Calculation of  $J$  From One Load-Displacement Curve for Three Point Bend Specimens," *Int. J. of Fracture* 12(5), 780-84 (October 1976).
14. J. D. Landes, H. Walker and G. A. Clarke, "Evaluation of Estimation Procedures Used in  $J$  Integral Testing," paper presented at the ASTM Committee E-24 Symposium on *Elastic-Plastic Fracture*, Atlanta, Georgia, Nov. 16-18, 1977.
15. G. A. Clarke and J. D. Landes, "Evaluation of  $J$  for the Compact Specimen," *J. of Testing and Evaluation* (to be published).
16. J. C. Newman, Jr., *Crack-Opening Displacements in Center-Crack, Compact, and Crack-Line Wedge-Loaded Specimens*, NASA TN D-8268, National Aeronautics and Space Administration, Langley Research Center, Hampton, Virginia (July 1976).
17. A. A. Wells, "The Status of COD in Fracture Mechanics," *Third Canadian Congress of Applied Mechanics*, University of Calgary, May 1971 (CANCAM 1971), pp. 59-77.
18. C. F. Boyle and A. A. Wells, *A Finite Element Study of Plane Strain Fracture Criteria Under Elastic-Plastic Conditions*, Department of Civil Engineering, Queen's University, Belfast, Ireland (June 1973).
19. J. D. Harrison, *A Comparison Between Four Elasto-Plastic Fracture Mechanics Parameters*, Report R/RB/E64/75, The Welding Institute, Cambridge, England (January 1975).
20. M. G. Dawes, "Elastic Plastic Fracture Toughness Based on the COD and  $J$  Integral Concepts," paper presented at the ASTM Committee E-24 Symposium on *Elastic-Plastic Fracture*, Atlanta, Georgia, Nov. 16-18, 1977.
21. J. G. Merkle, *An Elastic-Plastic Thick-Walled Hollow Cylinder Analogy for Analyzing the Strains in the Plastic Zone Just Ahead of a Notch Tip*, ORNL-TM-4071, Oak Ridge National Laboratory, Oak Ridge, Tennessee (January 1973).
22. J. A. Williams and W. J. Mills, "Assessment of the Ductile Fracture Toughness of Pressure Vessel Steel Using Small Specimens," pp. 29-37 in *Heavy Section Steel Technology Program Quarterly Progress Report for April-June 1977*, ORNL/NUREG/TM-147, Oak Ridge National Laboratory, Oak Ridge, Tennessee (December 1977).
23. R. H. Bryan et al., *Test of 6-In.-Thick Pressure Vessels. Series 3: Intermediate Test Vessel V-7B*, ORNL/NUREG-38, Oak Ridge National Laboratory, Oak Ridge, Tennessee (October 1978).
24. G. C. Smith, P. P. Holz, and W. J. Stelzman, *Crack Extension and Arrest Tests of Axially Flawed Steel Model Pressure Vessels*, ORNL/NUREG/TM-196, Oak Ridge National Laboratory, Oak Ridge, Tennessee (October 1978).

- 25. R. K. Nanstad and D. A. Canonico, "Liner and Penetration Studies," pp. 246-254 in *High Temperature Gas-Cooled Reactor Base Technology Program Annual Progress Report for Period Ending December 31, 1977*, ORNL-5412, Oak Ridge National Laboratory, Oak Ridge, Tennessee (July 1978).
- 26. D. M. Norris, Jr., J. E. Reaugh, B. Moran, and D. F. Quinones, *Computer Model for Ductile Fracture: Applications to the Charpy V-Notch Test*, EPRI NP-961, Lawrence Livermore Laboratory, Livermore, California (January 1979).
- 27. G. R. Odette, W. L. Server, W. Oldfield, R. O. Ritchie and R. A. Wullaert, *Analysis of Radiation Embrittlement Reference Toughness Curves*, FCC 78-11, Fracture Control Corporation, Goleta, California (Nov. 14, 1978).

Table 1. Asymptotic values of effective crack length at infinite displacement for compact specimens at limit load

| $a/W$ | $\alpha_e/W$ |             | $t/W$ |
|-------|--------------|-------------|-------|
|       | $B_0 = 3.5$  | $B_0 = 2.0$ |       |
| 0.3   | 0.682        | 0.702       | 0.738 |
| 0.5   | 0.766        | 0.775       | 0.791 |
| 0.7   | 0.855        | 0.858       | 0.863 |

Table 2. Precracked Charpy V-notch specimen data used for stable crack growth estimates\*

| Material                           | V-7B weld | V-7B weld | V-7B weld | W57-B.P. | W57-B.P. | W57-B.P. | W57-B.P. | W57-B.P. | W57-B.P. |
|------------------------------------|-----------|-----------|-----------|----------|----------|----------|----------|----------|----------|
| Spec. No.                          | V7W-4     | V7W-5     | V7W-17    | 57V-5    | 57V-6    | 57V-7    | 57V-8    | 57V-35   | 57V-36   |
| Test temp., °F                     | 150       | 200       | 200       | 100      | 200      | 300      | 0        | 200      | 0        |
| $\sigma_y$ , ksi                   | 70        | 70        | 70        | 66       | 63       | 63       | 70       | 63       | 70       |
| $W$ , in.                          | 0.3920    | 0.3934    | 0.3930    | 0.3930   | 0.3944   | 0.3941   | 0.3940   | 0.3942   | 0.3940   |
| $a$ , in.                          | 0.2054    | 0.1977    | 0.2160    | 0.2130   | 0.2136   | 0.2278   | 0.2053   | 0.2132   | 0.2182   |
| $b$ , in.                          | 0.1866    | 0.1957    | 0.1770    | 0.1800   | 0.1808   | 0.1663   | 0.1887   | 0.1810   | 0.1758   |
| $a/W$                              | 0.5240    | 0.5025    | 0.5496    | 0.5420   | 0.5416   | 0.5780   | 0.5211   | 0.5408   | 0.5538   |
| $P$ , lb                           | 1380      | 1560      | 1100      | 1220     | 1170     | 975      | 1410     | 1150     | 1210     |
| $\Delta$ , in.                     | 0.078     | 0.083     | 0.074     | 0.079    | 0.067    | 0.062    | 0.079    | 0.072    | 0.065    |
| $A$ , in.-lb                       | 83.04     | 111.96    | 69.36     | 81.36    | 65.28    | 50.28    | 94.68    | 71.16    | 66.24    |
| $J$ , in.-lb/in. <sup>2</sup>      | 2270.5    | 2908.5    | 1994.2    | 2300.3   | 1830.9   | 1534.4   | 2546.9   | 1994.7   | 1912.6   |
| $K_{IC}$ , ksi $\sqrt{\text{in.}}$ | 260.99    | 295.39    | 244.59    | 262.69   | 234.37   | 214.55   | 276.42   | 244.62   | 239.54   |
| $s$                                | 1.6701    | 1.8141    | 1.5977    | 1.6775   | 1.5511   | 1.4577   | 1.7360   | 1.5978   | 1.5748   |
| $m$                                | 6.0103    | 6.4422    | 5.7931    | 6.0325   | 5.6534   | 5.3732   | 6.2079   | 5.7934   | 5.7245   |
| $\delta$ , in.                     | 0.0054    | 0.0064    | 0.0049    | 0.0058   | 0.0051   | 0.0045   | 0.0059   | 0.0055   | 0.0048   |
| $\rho$ , in.                       | 0.0271    | 0.0306    | 0.0261    | 0.0287   | 0.0303   | 0.0288   | 0.0292   | 0.0299   | 0.0289   |
| $b_e/b$                            | 0.6481    | 0.5782    | 0.5868    | 0.5923   | 0.6004   | 0.6011   | 0.5882   | 0.5818   | 0.5937   |
| $\Delta a_e$ , in.                 | 0.0657    | 0.0825    | 0.0731    | 0.0734   | 0.0722   | 0.0663   | 0.0777   | 0.0757   | 0.0714   |
| $\Delta a$ , in.                   | 0.0385    | 0.0520    | 0.0470    | 0.0446   | 0.0420   | 0.0375   | 0.0485   | 0.0458   | 0.0425   |
| $m_0$                              | 2.4826    | 2.3860    | 2.0687    | 2.3626   | 2.3680   | 2.3339   | 2.3355   | 2.2900   | 2.3136   |

\*Conversions:

$^{\circ}\text{C} = 5/9 (\text{ }^{\circ}\text{F} - 32)$ ;

1 ksi = 6.8948 MPa;

1 in. = 25.4 mm;

1 lb = 4.4482 N;

1 in.-lb = 0.1130 J;

1 in.-lb/in.<sup>2</sup> = 0.17513  $\text{KJ}\cdot\text{m}^{-2}$ ;

1 ksi  $\sqrt{\text{in.}}$  = 1.0988  $\text{MN}\cdot\text{m}^{-3/2}$ .

Table 3. Compact specimen data used for stable crack growth estimates ( $B_0 = 3.5$ )\*

| Material                           | A508-1 | A537-1 | A537-2 | A537-1 | A537-1 |
|------------------------------------|--------|--------|--------|--------|--------|--------|--------|--------|--------|--------|--------|
| Spec. No.                          | 02T3F1 | 02C1P1 | 01C3P1 | 02COP1 | 01C6P2 | 01E7P2 | 01C3P2 | 01C4P2 | 01E4P4 | 02A4P1 | 03A6P1 |
| Test temp., °F                     | 71.6   | 64.4   | 212    | 32     | 32     | 77     | 64.4   | 212    | 32     | 167    | 302    |
| $\sigma_y$ , ksi                   | 50.7   | 52.2   | 56.5   | 52.2   | 55.8   | 58.7   | 54.8   | 52.9   | 60.0   | 50     | 45     |
| $B$ , in.                          | 0.9972 | 1.0003 | 1.0004 | 1.0003 | 1.0005 | 0.9996 | 1.0004 | 1.0004 | 1.0003 | 0.3944 | 0.3946 |
| $W$ , in.                          | 1.9964 | 2.000  | 2.0008 | 2.0013 | 2.0020 | 2.0021 | 2.0013 | 2.0024 | 2.0045 | 0.7896 | 0.7887 |
| $a$ , in.                          | 1.0764 | 1.0839 | 1.0819 | 1.0668 | 1.0490 | 1.0345 | 1.0468 | 1.0506 | 1.0477 | 0.431  | 0.450  |
| $b$ , in.                          | 0.9200 | 0.9161 | 0.9189 | 0.9345 | 0.9530 | 0.9676 | 0.9545 | 0.9518 | 0.9568 | 0.359  | 0.339  |
| $z$ , in.                          | 0      | 0      | 0      | 0      | 0      | 0      | 0      | 0      | 0      | 0.2645 | 0.2631 |
| $a/W$                              | 0.5392 | 0.5420 | 0.5407 | 0.5331 | 0.5240 | 0.5167 | 0.5231 | 0.5247 | 0.5227 | 0.5458 | 0.5706 |
| $z/W$                              | 0      | 0      | 0      | 0      | 0      | 0      | 0      | 0      | 0      | 0.3350 | 0.3336 |
| $P$ , 1b                           | 12,525 | 13,000 | 12,000 | 13,350 | 15,000 | 15,500 | 14,900 | 13,700 | 16,400 | 2055   | 1670   |
| $\Delta_g$ , in.                   |        |        |        |        |        |        |        |        |        | 0.1800 | 0.1532 |
| $\Delta_L$ , in.                   | 0.2153 | 0.1698 | 0.1885 | 0.1909 | 0.1813 | 0.1714 | 0.1783 | 0.1987 | 0.1961 |        |        |
| $A^†$ , in.-1b                     | 2339   | 1899.4 | 1937.2 | 2212.7 | 2303.5 | 2258.4 | 2262.7 | 2347.9 | 2732.8 | 322.6  | 220.1  |
| $a_e/W$                            | 0.7474 | 0.7467 | 0.7447 | 0.7445 | 0.7329 | 0.7301 | 0.7340 | 0.7384 | 0.7331 | 0.7522 | 0.7616 |
| $\Delta_L/\Delta_g$                | 1.0    | 1.0    | 1.0    | 1.0    | 1.0    | 1.0    | 1.0    | 1.0    | 1.0    | 0.6919 | 0.6954 |
| $J$ , in.-1b/in. <sup>2</sup>      | 5681   | 4615   | 4694   | 5282   | 5403   | 5232   | 5301   | 5514   | 6388   | 3511   | 2532   |
| $K_{Ic}$ , ksi $\sqrt{\text{in.}}$ | 412.8  | 372.1  | 375.2  | 398.1  | 402.6  | 396.2  | 398.8  | 406.7  | 437.8  | 324.5  | 275.6  |
| $s$                                | 2.240  | 2.10   | 2.11   | 2.19   | 2.21   | 2.18   | 2.19   | 2.22   | 2.32   | 1.928  | 1.73   |
| $m$                                | 7.72   | 7.31   | 7.34   | 7.57   | 7.62   | 7.55   | 7.58   | 7.66   | 7.96   | 6.785  | 6.20   |
| $\delta$ , in.                     | 0.0145 | 0.0121 | 0.0113 | 0.0134 | 0.0127 | 0.0118 | 0.0128 | 0.0136 | 0.0134 | 0.0103 | 0.0091 |
| $p/W$                              | 0.0504 | 0.0532 | 0.0447 | 0.0521 | 0.0514 | 0.0503 | 0.0525 | 0.0506 | 0.0500 | 0.0625 | 0.0649 |
| $\Delta\alpha$ , in.               | 0.315  | 0.303  | 0.319  | 0.319  | 0.315  | 0.327  | 0.317  | 0.327  | 0.321  | 0.114  | 0.099  |
| $m_0$                              | 1.87   | 1.90   | 1.61   | 1.87   | 1.87   | 1.78   | 1.89   | 1.81   | 1.89   | 2.05   | 2.11   |

\*Conversions:

 $^{\circ}\text{C} = 5/9 (\text{ }^{\circ}\text{F} - 32)$ ;

1 ksi = 6.8948 MPa;

1 in. = 25.4 mm;

1 lb = 4.4482 N;

1 in.-1b = 0.1130 J;

1 in.-1b/in.<sup>2</sup> = 0.17513  $\text{KJ} \cdot \text{m}^{-2}$ ;1 ksi  $\sqrt{\text{in.}} = 1.0988 \text{ MN} \cdot \text{m}^{-3/2}$ .

<sup>†</sup> $A$  is the area under the measured load-displacement curve. If the measured displacement is  $\Delta_g$ , then the area listed is  $A_g$ .

## FIGURE CAPTIONS

Fig. 1. Graphical determination of coefficients in the approximate expression for  $J$  for a compact specimen.

Fig. 2. Comparison between approximate and theoretical boundary collocation values of the non-dimensional compliances, at the crack mouth and load line, for a compact specimen.

Fig. 3. Estimated loads at a displacement of 2 mm (0.08 in.) for a series of 22.9 mm (0.90 in.) thick, blunt notched 1T profile compact specimens of HY 130 steel with various  $a/W$  ratios (experimental data from Ref. 14).

Fig. 4. Geometric definitions for the compact specimen at limit load.

Fig. 5. Dimensions characterizing the crack profile model used for analysis.

Fig. 6. Comparison of calculated values of  $J$  and  $\Delta a$  at maximum load for several monotonically loaded precracked Charpy V-Notch and compact specimens of various pressure vessel steels, with a reference curve for A533, grade B, class 1 steel.

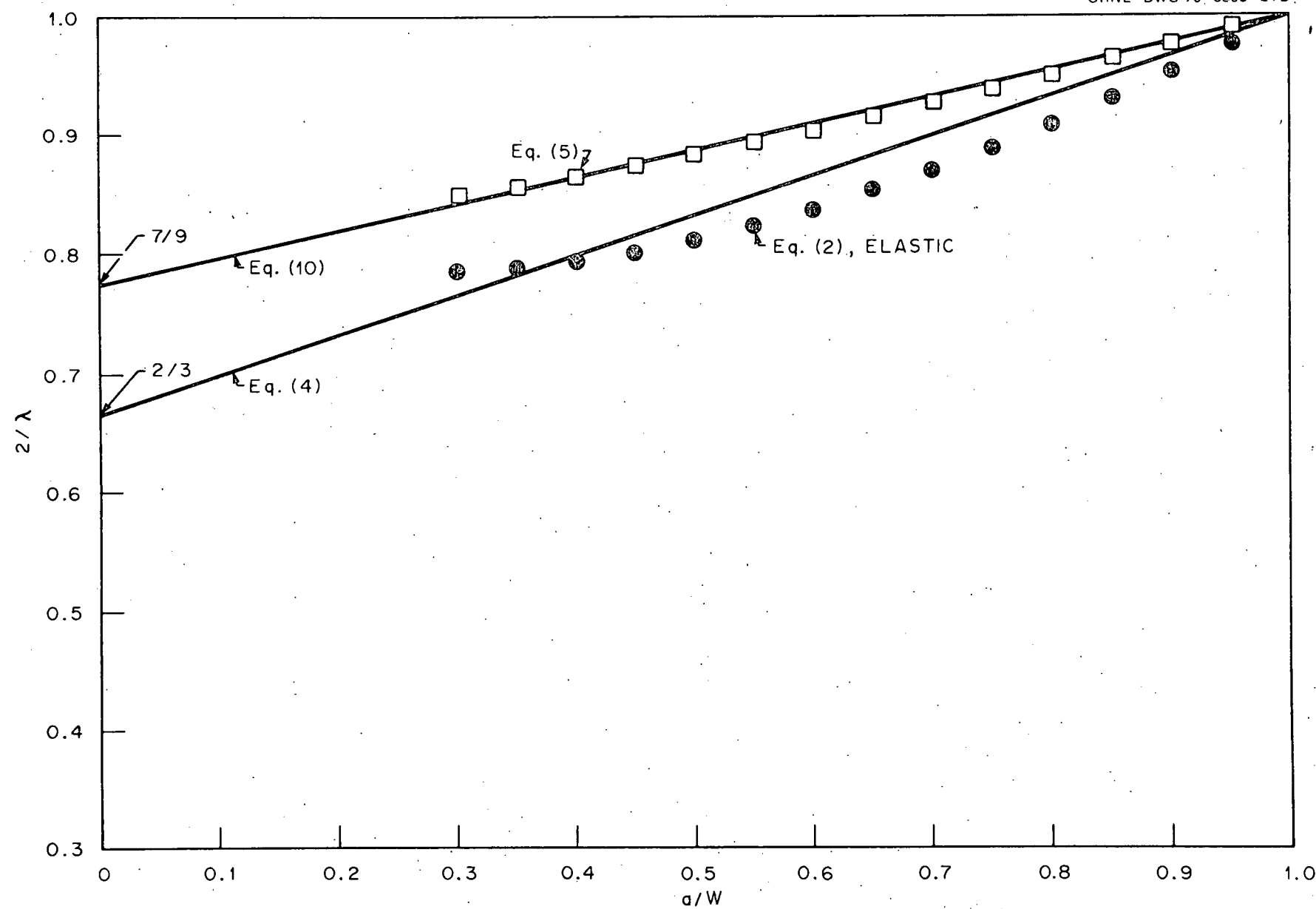


FIGURE 1

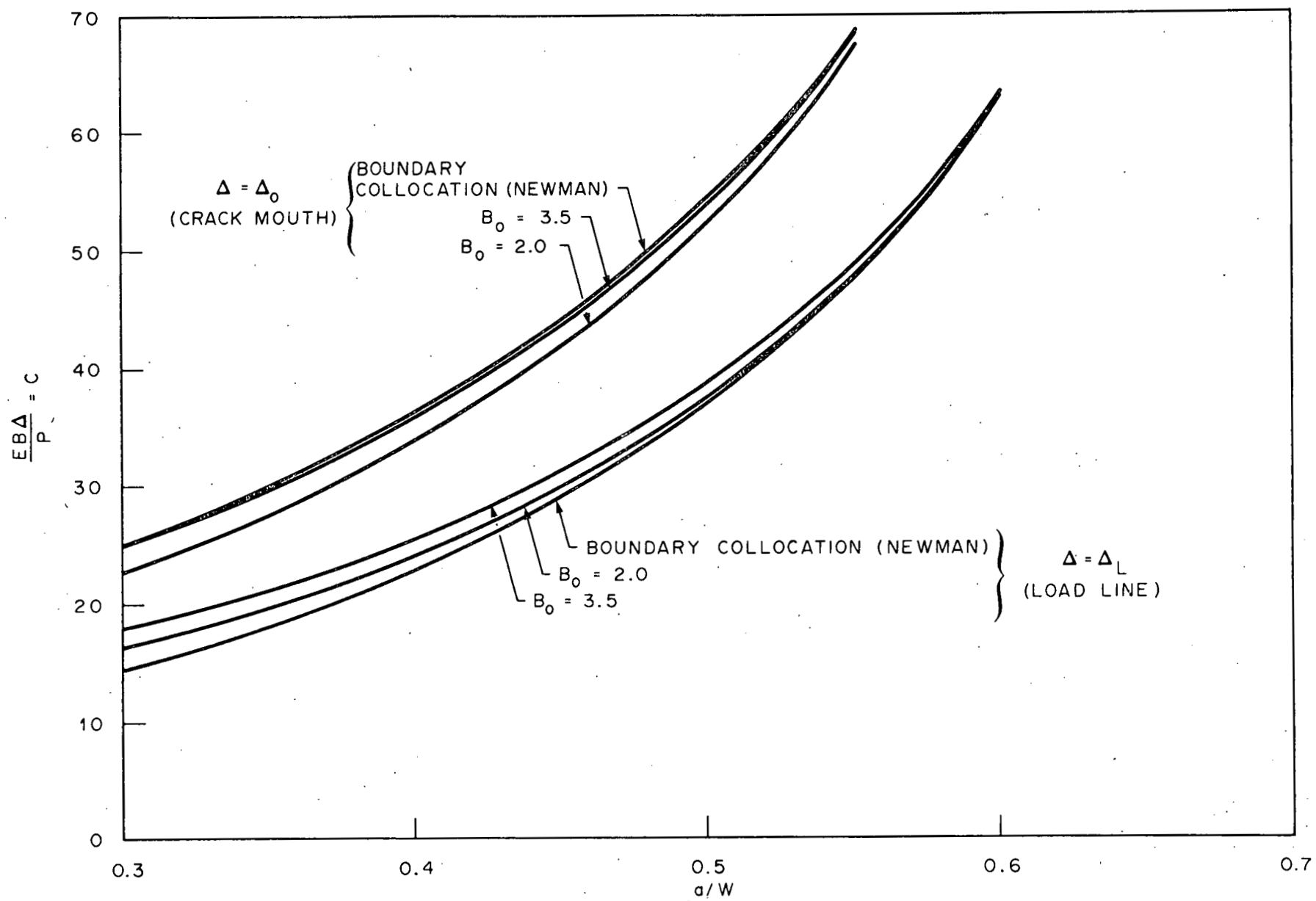


FIGURE 2

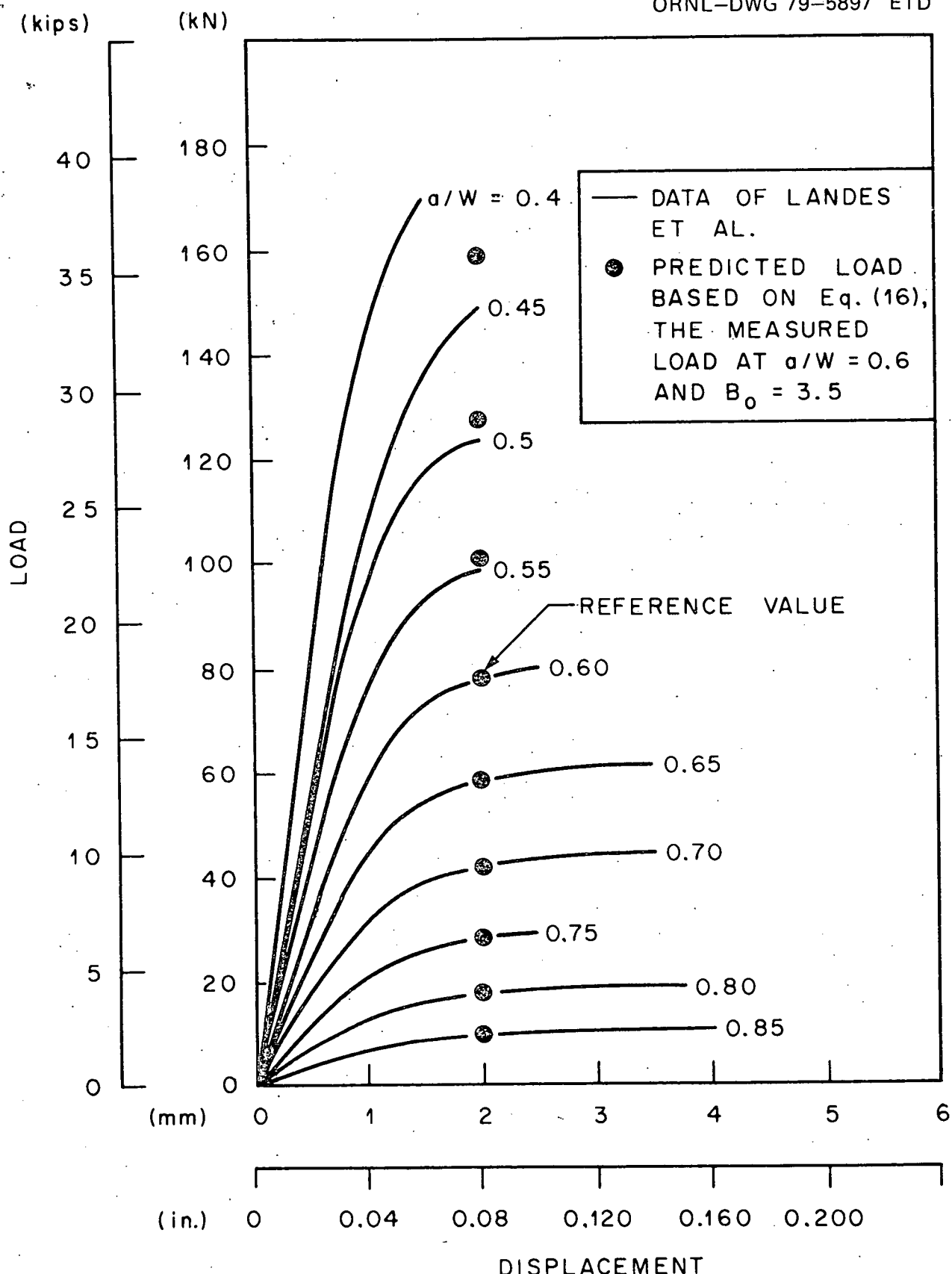
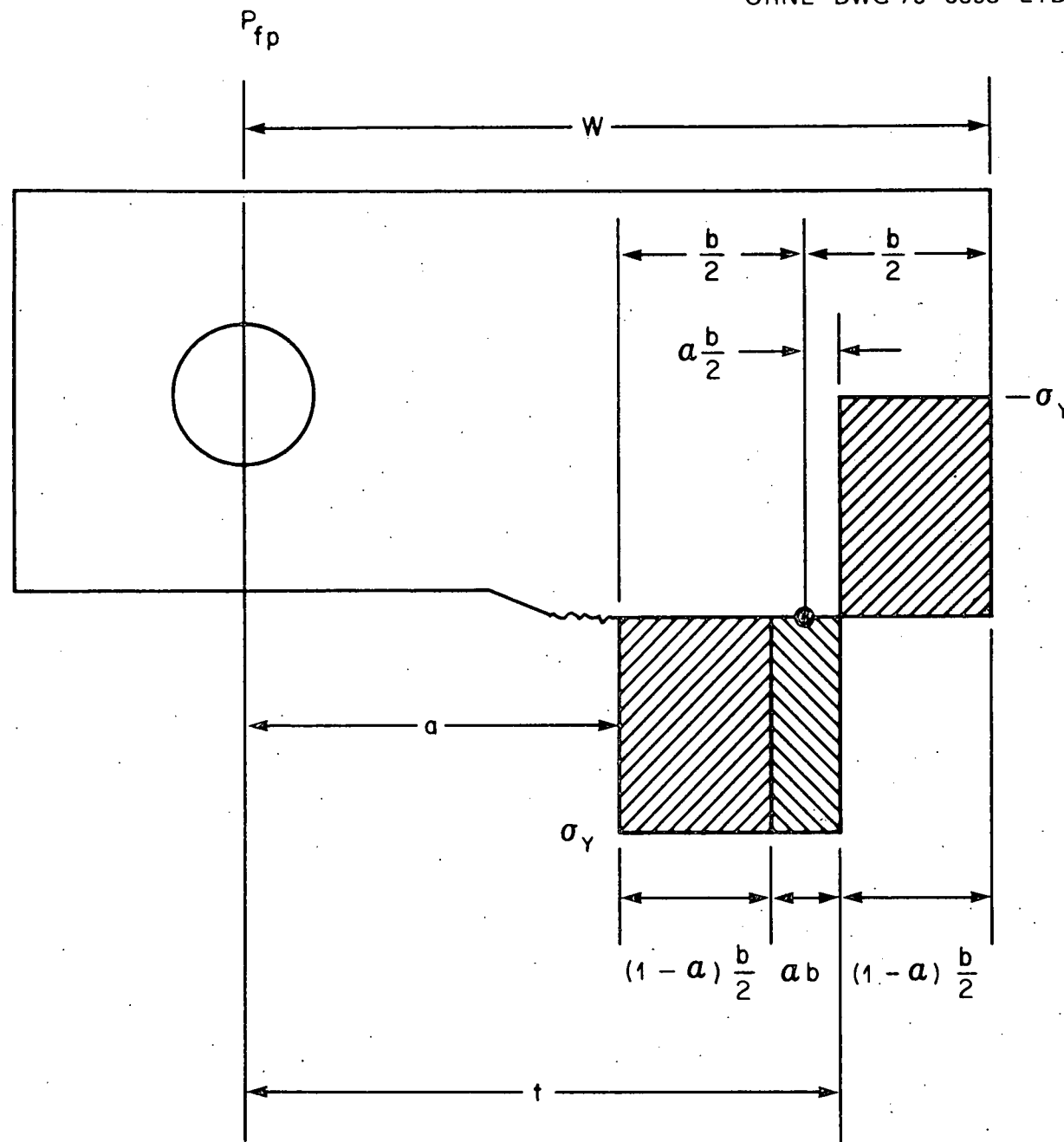


FIGURE 3



## FIGURE 4

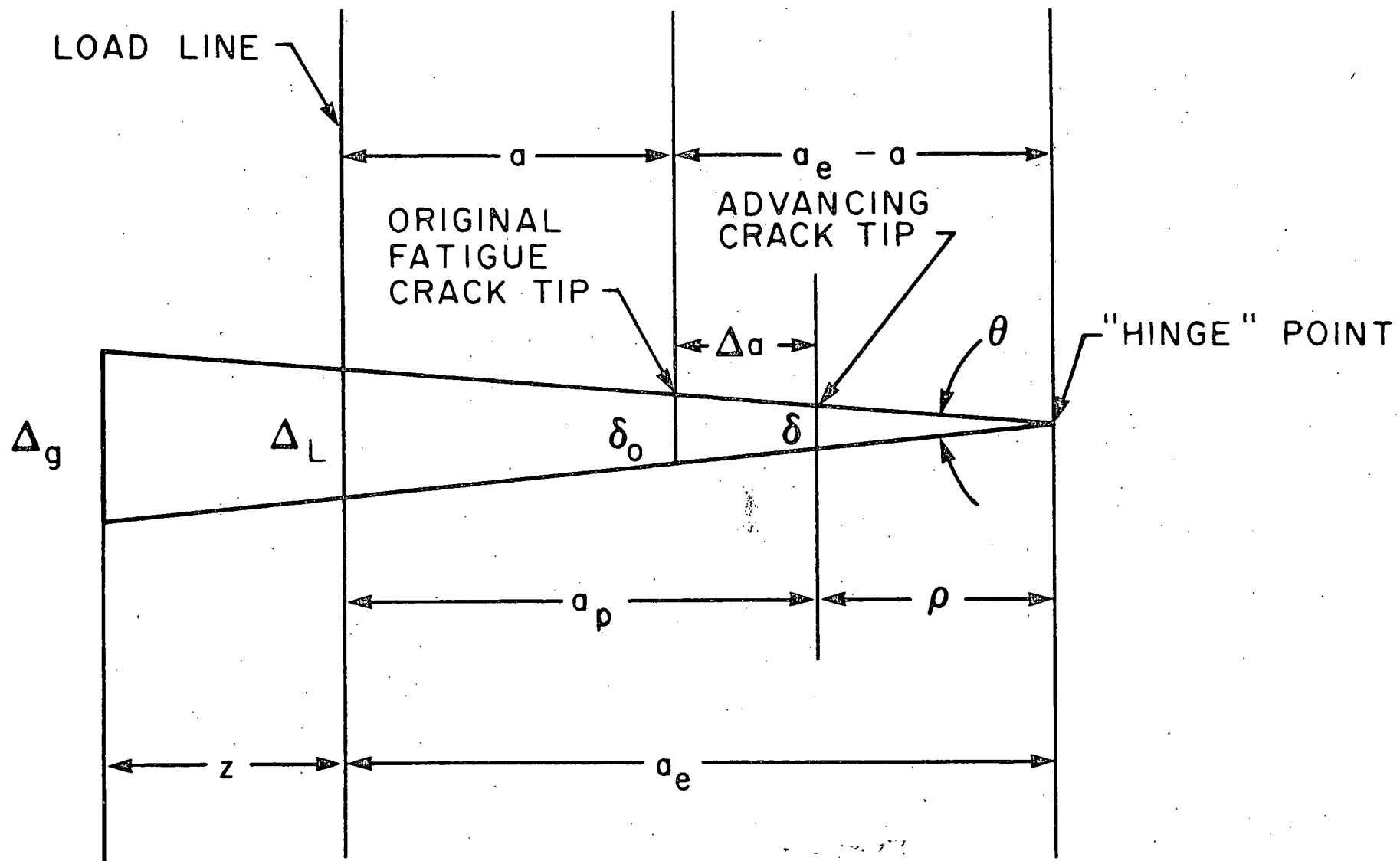


FIGURE 5

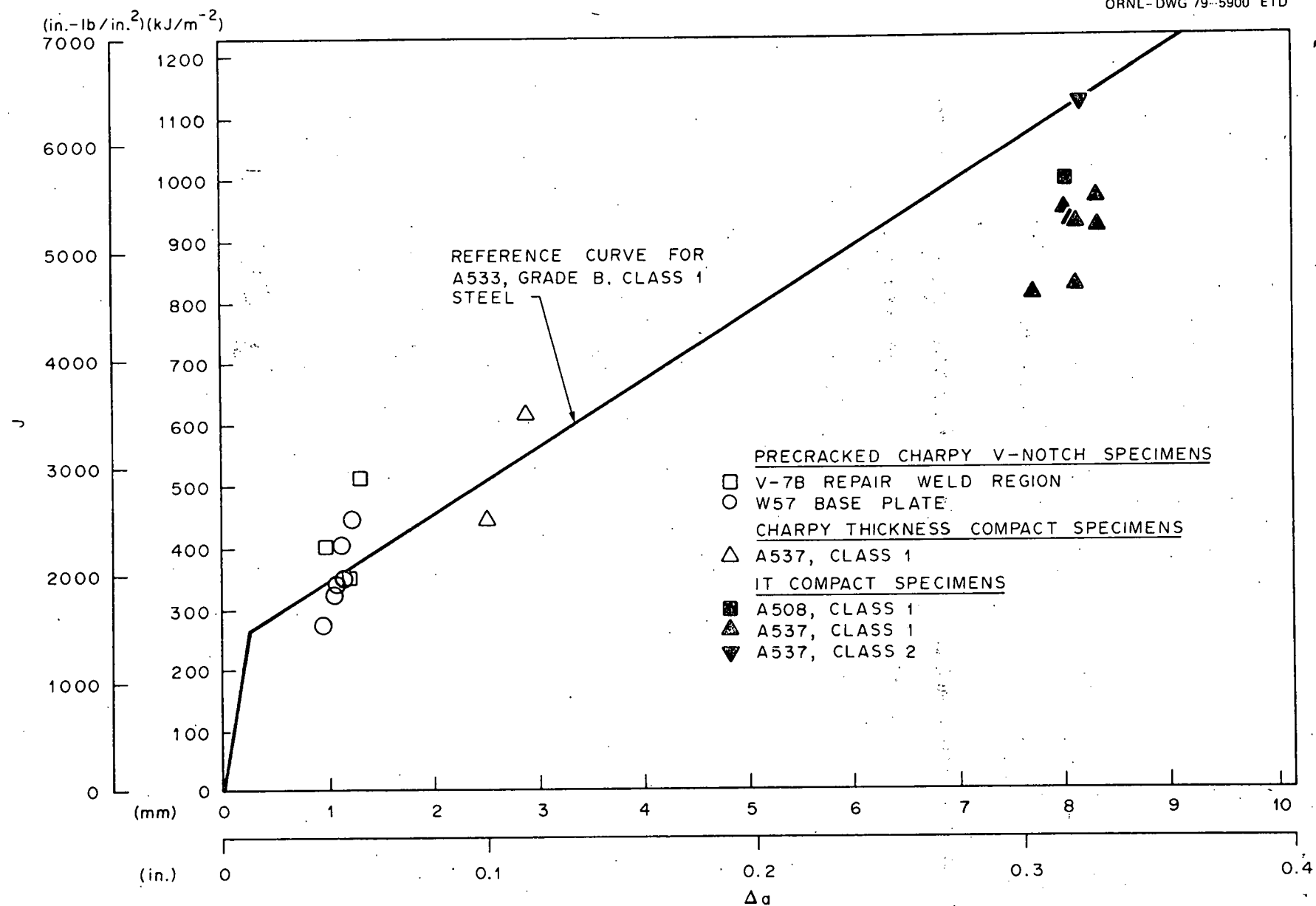


FIGURE 6